

Electronic Supplementary Information

Enhanced magnetic and thermoelectric properties of epitaxial polycrystalline SrRuO₃ thin film

Sungmin Woo^{a,b}, Sang A Lee^a, Hyeona Mun^c, Young Gwan Choi^d, Chan June Zhung^d, Soohyeon Shin^a, Morgane Lacotte^e, Adrian David^e, Wilfrid Prellier^e, Tuson Park^a, Won Nam Kang^a, Jong Seok Lee^d, Sung Wng Kim^c, and Woo Seok Choi^{a*}

^aDepartment of Physics, Sungkyunkwan University, Suwon, 16419, Korea

^bCenter for Integrated Nanostructure Physics, Institute for Basic Science, Suwon, 16419, Korea

^cDepartment of Energy Sciences, Sungkyunkwan University, Suwon 16419, Korea

^dDepartment of Physics and Photon Science, Gwangju Institute of Science and Technology, Gwangju 61005, Korea

^eLaboratoire CRISMAT, CNRS UMR 6508, ENSICAEN, Normandie Université, 6 Bd Marechal Juin, F-14050 Caen Cedex 4, France

*e-mail: choiws@skku.edu.

Epitaxial relationship between single-crystalline SrRuO₃ thin films and SrTiO₃ substrate

Figure S1 indicates that (100), (110), and (111) oriented single-SRO thin films are grown epitaxially without any strain relaxation. The reciprocal space maps clearly show that the thin films are fully strained.

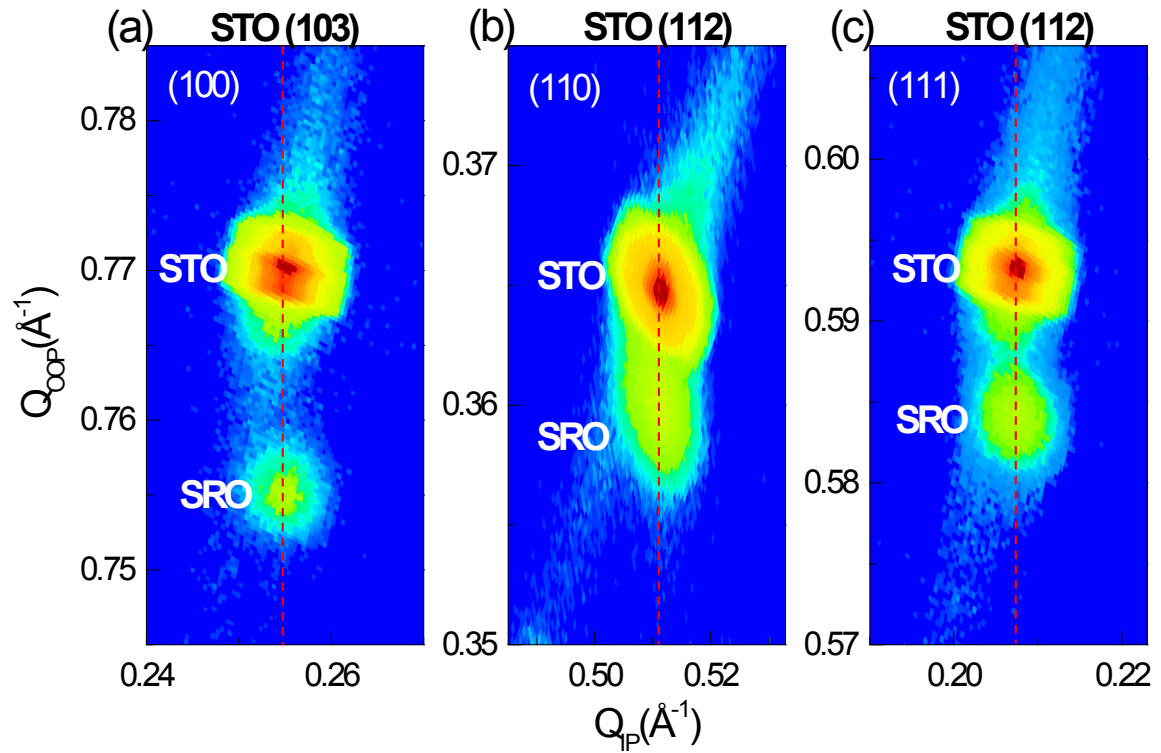


Figure S1. XRD reciprocal space maps of 30-nm-thick single-crystalline SrRuO₃ thin films. (a) (103) Bragg reflection of the SrTiO₃ substrate for (100) SrRuO₃ thin film. (b) (112) Bragg reflection of the SrTiO₃ substrate for (110) SrRuO₃ thin film. (c) (112) Bragg reflection of the SrTiO₃ substrate for (111) SrRuO₃ thin film.

Epitaxial orientation relationship between polycrystalline SrTiO₃ substrate and SrRuO₃ thin film

Using Electron backscattering diffraction (EBSD), we obtained the epitaxial orientation relationship between the polycrystalline SrTiO₃ substrate and SrRuO₃ thin film (Fig. S2). Note that here we used thick (300 nm) SrRuO₃ film to obtain reliable signal of the film from the EBSD measurements. The colours for the substrate and the thin film indicated by the inverse pole figure are not exactly the same, because of the experimental and analysis error. In particular, the significant difference in the electric resistivity between the substrate (insulator) and the film (metal) results in difference in the backscattering rate of the electrons. Nevertheless, the overall orientation can be considered to be highly alike, judging from the cube representation of the orientation shown in Figure S2. Therefore, we can conclude that the grains in the polycrystalline thin film and substrate have the same orientation.

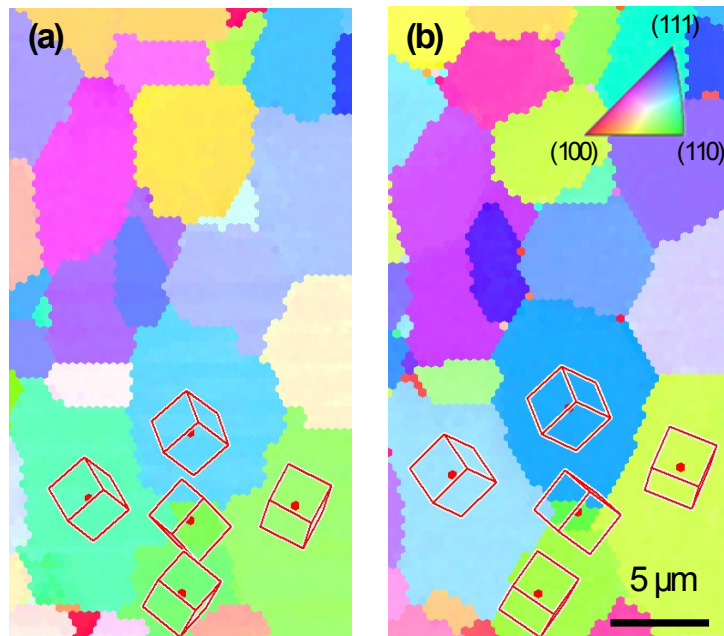


Figure S2. Inverse pole figure images of substrate (a) and film (b). Each corresponding domain in polycrystalline film followed substrate orientations. The cubic in each grain represent schematic orientation information.

Metallic behavior of single- and polycrystalline SrRuO₃ epitaxial thin films in different temperature ranges

To investigate the temperature dependence of the metallic behaviour of single- and poly-SRO thin films, the $\rho(T)$ curves (Fig. S3) were fitted using the relation $\rho(T) = \rho_0 + AT^\alpha$ (where ρ_0 is the residual resistivity, A is a coefficient, and α is scaling parameter), in three different temperature ranges: $T < 30$ K, $30 \text{ K} < T < T_C$, and $T_C < T$. Different α exponents were used to fit the metallic behaviour of the $\rho(T)$ curves in each region ($\alpha = 2$ for $T < 30$ K, $\alpha = 1.5$ for $30 \text{ K} < T < T_C$, and $\alpha = 2.0$ for $T_C < T$).

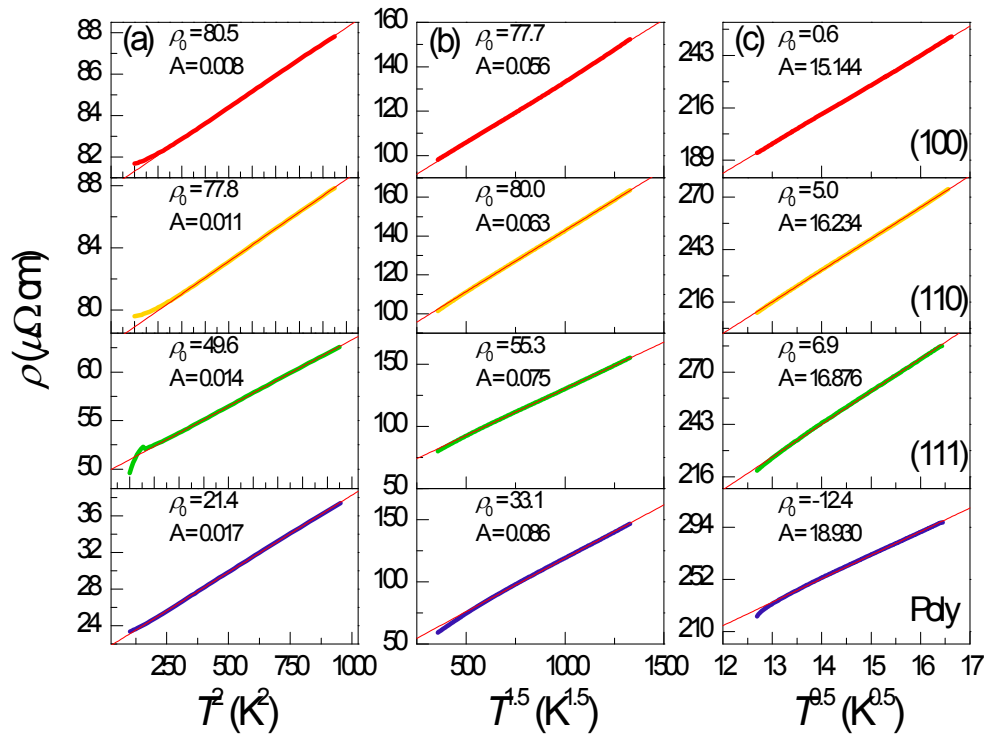


Figure S3. Temperature dependence of $\rho(T)$ for single- and polycrystalline SrRuO₃ thin films in three specific regions (a) T^2 for $T < 30$ K, (b) $T^{1.5}$ for $30 \text{ K} < T < T_C$, and (c) $T^{0.5}$ for $T_C < T$. The thick and thin lines represent the experimental data and the fitted results, respectively.

Relationship between atomic average distance and T_C

The average distances between the Ru ions can be deduced from simple structural considerations. Taking into account the different strain state of single-crystalline thin films with different orientation, we obtained the Ru-Ru average distances between nearest, next-nearest, and next-next-nearest neighbour (n.n., n.n.n., and n.n.n.n., respectively) Ru ions, as shown in Figure S4. As the average atomic distance increases, the ferromagnetic T_C decreases, as expected.

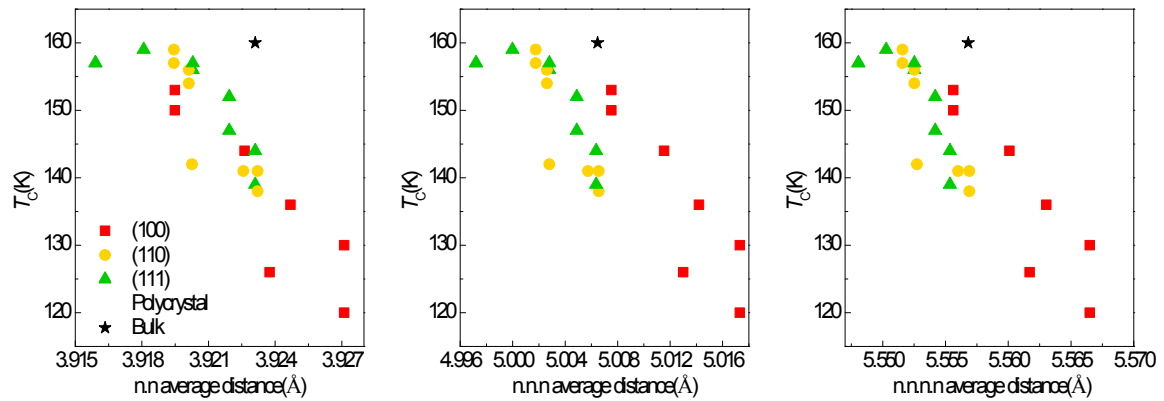


Figure S4. Dependence of T_C on Ru-Ru average distance, calculated for (a) n.n., (b) n.n. and n.n.n., and (c) n.n., n.n.n., and n.n.n.n. Ru ions. The corresponding number of Ru ions included in the calculation increases from (a) 6 to (b) 18 to (c) 26. The same trend was obtained when different number of Ru ions was considered.

XRD analysis of epitaxial single- and polycrystalline SrRuO₃ thin films

Figure S5 shows the XRD θ - 2θ scans for epitaxial poly-SRO thin film. The comparison of the thickness dependence of the single- and poly-SRO thin films indirectly indicates that the poly-SRO film is strained with respect to the substrate lattice, and also that its strain state is not identical to that of the single-SRO thin film. Compared with the single-SRO thin film, the poly-SRO thin film has a smaller c -axis lattice constant, suggesting a lower compressive strain, possibly due to the coalescence of the grains. An even smaller c -axis lattice constant is observed for the thicker film, indicating further strain relaxation.

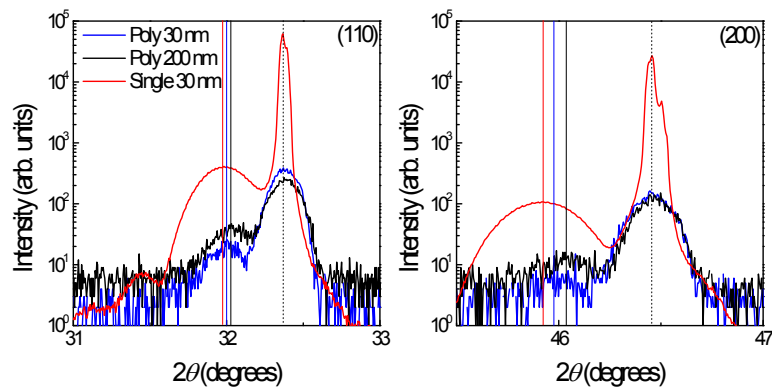


Figure S5. Comparison between epitaxial single- and poly-crystalline SrRuO₃ thin films for (a) (110) and (b) (200) XRD Bragg peaks, describing the evolution of strain in the SrRuO₃ thin films.